Natural draft and forced primary air combustion properties of a top-lit up-draft research furnace

Thomas Kirch*, Paul R. Medwell, Cristian H. Birzer

School of Mechanical Engineering, The University of Adelaide, S.A. 5005, Australia

Abstract

Worldwide, over four million people die each year due to emissions from cookstoves. To address this problem, advanced cookstoves are being developed, with one system, called a top-lit up-draft (TLUD) gasifier stove, showing particular potential in reducing the production of harmful emissions. A novel research furnace analogy of a TLUD gasifier stove has been designed to study the TLUD combustion process. A commissioning procedure was established under natural draft and forced primary air conditions. A visual assessment was performed and the temperature and emissions profiles were recorded to identify the combustion phases. The efficiency was evaluated through the nominal combustion efficiency (NCE = $CO_2/(CO_2 + CO)$), which is very high in the migrating pyrolysis phase, averaging 0.9965 for the natural draft case. Forced primary air flows yield similar efficiencies. In the lighting phase and char gasification phase the NCE falls to 0.8404 and 0.6572 respectively in the natural draft case. When providing forced primary air flows, higher NCE values are achieved with higher air flows in the lighting phase, while with lower air flows in the char gasification phase. In the natural draft case high H_2 emissions are also found in the lighting and char gasification phases, the latter indicating incomplete pyrolysis. From the comparison of the natural draft with the forced draft configurations, it is evident that high efficiency and low emissions of incomplete combustion can only be achieved with high controllability of the air flow in the different phases of combustion.

Keywords:
Top-lit up-draft, Natural draft, Gasification, Pyrolysis, Cookstove

*Corresponding author

Email addresses: thomas.kirch@adelaide.edu.au (Thomas Kirch), paul.medwell@adelaide.edu.au (Paul R. Medwell), cristian.biryer@adelaide.edu.au (Cristian H. Birzer)

1. Introduction

Energy consumption in private households in developing countries is still primarily based on biomass fuels. This directly affects 2.7 billion people [1] who rely on traditional cooking methods, which typically have a very low efficiency and produce harmful emissions through incomplete combustion. This results in approximately 4.3 million premature deaths worldwide each year from cooking-related illnesses caused by household air pollution [2]. In order to achieve substantial health benefits, cleaner burning cookstoves than are currently in widespread use are needed [3, 4]. One type of cookstove that has been recognised as potentially able to achieve this goal are "gasifier" stoves [5]. These stoves force volatile gases out of a solid fuel and burn them separately from the solid body [6]. This can reduce harmful emission production; however, there is a lack of scientific understanding to enable stove optimisation.

Gasifier cookstoves can be distinguished by the direction of the gasification air. Available designs of cookstoves use either updraft, downdraft or inverted downdraft, also called top-lit up-draft (TLUD), flow [7]. A TLUD stove is investigated in this study. To operate as a TLUD, the stove is filled with batches of fuel and lit from the top. Firstly, the top layer of biomass is ignited, typically by a kindling material, before a pyrolytic front forms, which moves downwards, opposite to the gas flow, through the fuel-stack, as illustrated in Figure 1. In the enclosed space of the stove, the oxygen is quickly consumed in the oxidation process of the lighting phase. The heat released from the top layer causes lower layers to pyrolyse, which means that volatile matter is released from the fuel in an inert atmosphere [8]. This process is called a migrating pyrolytic front [9], which moves, in relation to the primary air, down the fuel-stack [10]. The pyrolysis products are liquids (water, heavier hydrocarbons, and tars), gases (such as CO, CO_2, or CH_4) and solid char [11]. The pyrolytic front is sustained by simultaneous gasification, in which the pyrolysis products can partially oxidise with the primary air into gases (CO, CO_2, H_2 and lesser quantities of hydrocarbon gases) [12]. In inverted downdraft gasifiers, heavier hydrocarbons and the liquid tar can crack into lighter components as they move through the high temperature zone of the char layer[10, 13]. This process is highly complex, in part due to the thin char layer [14], and therefore the scientific understanding of these reactions in TLUD stoves is limited. Greater scientific understanding of the tar cracking processes for TLUD stoves is needed to ensure optimisation of

systems in terms of emissions production.

The combustible pyrolysis products leave the fuel-stack at temperatures of ≈ 600 °C [15], and are mainly composed of CO, H_2, CH_4 and some heavier hydrocarbons (C_xH_y) [16]. Once these gases reach the secondary air inlet, they are mixed with air and can be combusted if an ignition source is present, as shown in Figure 1. As a result of gas-combustion and compared with other cookstoves, gasifier stoves have been shown to produce low CO and particulate matter (PM) emissions under laboratory conditions [17, 18]. It has been shown that variations in the stove geometry and the utilized fuel have a significant impact on the stove's performance [19, 20]. It has been observed that the heat transfer, to a vessel on the stove, is a strong function of the vessel diameter, while swirl of secondary air has a negligible impact [14]. It is clear that the design of the stove to optimise gas production for combustion, and for subsequent heat transfer are limited.

From the pyrolysis processes, char remains as a solid product. The char yield is mainly dependent on the superficial velocity, which is determined by the gas flow over the cross-sectional area [10] and the moisture content of the biomass [21, 22]. This char can be further gasified and combusted in the stove or, if no further air is supplied and the oxidation process is quenched, it can be collected. If collected, the char can be used as either fuel or as a soil amendment (termed biochar). When using it as a soil amendment, the whole process could be seen as a mechanism for carbon sequestration [19, 23]. If the quenching process is not conducted early enough, the char can continue to burn, producing high levels of harmful emissions, as well as produce ash, which cannot be used as a solid enhancer. It is therefore necessary to further develop the understanding of quenching of char for subsequent use, or for improved combustion in a process beneficial to the end user.

Uncertainty in the existing results is exacerbated by the influence of different standardised tests and kindling materials on the performance of TLUD cookstoves. Arora *et al.*assessed different test protocols, and determined that, for given conditions, the emissions factors, (primarily of CO and PM), varied leading to differences in the cookstove performance. Wood, mustard stalks and kerosene were tested as kindling materials and it was observed that CO peaks would increase with lower calorific values of the kindling materials [24]. All of these studies have evaluated specific designs and analysed their performance while performing cooking tasks.

The previous paragraphs show that there are many gaps in scientific understanding of basic TLUD operation and design. These unknowns are ex-

tended when considering various fuel types and fuel quantities. Additionally, it is also known that these stoves can be used under natural draft conditions or with the assistance of a fan that creates a forced airflow. Altering the available flow rates can be beneficial, or detrimental, to the combustion processes. How these modifications influence the heat transfer, emissions production and burn rates are all crucial in development improved cookstoves and thus helping increase the quality of life for billions of people. However, much of the research has been conducted on stoves that do not allow for modification of these aspects. It is for this reason that a TLUD analogous furnace has been developed to allow for systematic studies of TLUD combustion. What is not completely known is how accurate the analogy is across all aspects of TLUD stove design.

The aim of the current paper is to present results from commissioning a TLUD analogy furnace and determine if forced draft flows can be used to simulate natural draft. Specifically, the study includes analysis of emissions and temperature profiles in natural draft as well as forced primary air TLUD operation, in order to characterise, understand and evaluate subsequent combustion processes.

2. Materials and Methods

The research furnace, previously presented in Kirch et al. [25], was revised as a TLUD stove with the general characteristics of a primary air inlet at the bottom of the furnace, and a lateral secondary air inlet in the upper region. The furnace's dimensions were chosen to be larger than most extant commercial products and stoves in order to address scaling issues and achieve greater variability of the adjustable parameters. The furnace enables various combustion-relevant parameters to be controlled. The increased size of the research furnace allows the amount and location of the fuel to be widely altered which in turn permits the scaling from use in private households to use in communal kitchens to be studied, although this is outside the scope of the present study. The principal components of the research furnace are a stove body, a primary air inlet chamber and a secondary air inlet stove extension, which are shown in Figure 2.

2.1. The TLUD research furnace

The central component of the research furnace is a 600-mm-tall steel cylinder with an inner diameter of 206 mm and 8 mm wall thickness, illus-

trated in Figure 2. Inside the stove body, a grate is located, which holds the fuel-stack in place. The circular grate is perforated with 3-mm-diameter holes, with 26% open-area ratio. This allows air from beneath the grate to enter the fuel-stack. The fuel grate is located 420 mm below the top of the stove body and is easily removable for post-combustion analysis of the solid residual matter, as well as cleaning. The steel cylinder, in combination with the fuel grate, forms the stove body. It is placed on top of a steel frame that serves as the primary air inlet chamber.

The steel frame of the primary air inlet chamber has the following dimensions: 248 mm × 248 mm × 150 mm (length × width × height). The frame allows all sides to be closed off, so that air can be applied through only one inlet. The inlet can be connected to compressed air and the airflow is controlled by a needle valve and a rotameter. If the sides are not closed off, air enters freely.

The secondary air inlet is provided by a detachable stove extension to the top of the stove body. This extends the furnace height by 340 mm and is equipped with three 20 mm wide and 190 mm long lateral air inlets. The centre line of the air inlets is situated 55 mm above the top of the stove body as shown in Figure 2. In all the tested configurations the secondary air inlets are unobstructed which allows secondary air to enter via natural draft induced by buoyancy.

2.2. Set-up of the data collection

Emissions data were collected at one central location while the temperature data were constantly measured at two locations. For emissions testing, the research furnace was placed under a hood, which was, in turn, attached to an extraction duct and a fan. The measuring probe of a Testo 350XL gas analyser was placed in the centre of the fume hood inlet at a distance of 830 mm above the exit plane of the research furnace extension, as presented in Figure 3. The probe is located in the centre of the collection area of the fume hood and thus in the focus point of the emissions from the stove. The Testo 350XL was used to record the CO, CO_2 and H_2 concentrations at an interval of 1 Hz, on a dry basis. The resolution was 1 cm^3 m^{-3} for low emission levels (<2000 cm^3 m^{-3}) and 5 cm^3 m^{-3} for high emission levels (>2000 cm^3 m^{-3}) of CO measurements. The resolution for CO_2 measurements was 0.01%.

A normalisation process was performed for all the gathered emissions concentrations. This was necessary because the quantitative measurements

were taken at a location of 830 mm above the stove, where flue gas from the combustion process is mixed with the surrounding air. The emissions data are related to the sum of all carbon emissions, here CO and CO_2. Other carbon-containing species were below the detection limits of the apparatus. Various emissions are each normalised with respect to the sum of the carbon emissions, because these can be attributed to the combustion process and provide the key relationship between the intensity of the combustion process and the release of certain products.

The temperature data were collected constantly via two K-type thermocouples, at locations A and B, and, when needed, via an infra-red thermometer at location C on the outer surface of the stove body. Both thermocouples were positioned in the centre of the stove body, as illustrated in Figure 3. Location A, above the secondary air inlet, was chosen because it is expected to detect high temperatures when pyrolysis products burn with the secondary air inside the stove extension. The thermocouple at location B, in the stove body, is closer to the fuel-stack. Therefore it can capture when combustion occurs at the fuel-stack and can measure the temperature of the pyrolysis products during the migrating pyrolysis phase. The infra-red thermometer is used to measure the outside wall temperature of the stove, which is needed for the testing procedure, presented in Section 2.3.

2.3. The commissioning process

A testing procedure was established for the research furnace. To account for the influence of the thermal mass of the research furnace, with its wall thickness of 8 mm, on the combustion performance, it was ensured that the furnace is either pre-heated, or starts cold. For each test, a batch of 700 g of fuel was placed on the fuel grate and evenly distributed to achieve a level surface. The furnace was run once to pre-heat. Then for the pre-heated tests, which are presented here, the furnace was re-fuelled when the outer wall temperature at location C (see Figure 3) reached 150 °C. As kindling material, approximately 5 mL of methylated spirits (96% ethanol) was poured evenly over the fuel. When the outer wall temperature at location C measured 135 °C a lit paper towel (approximately 190 mm × 100 mm) was dropped into the furnace to ignite the kindling material. The initial temperatures were chosen for the commissioning process to prevent volatilisation in the fuel, which starts at approximately 200 °C [26]. Data were recorded until only ash was left on the fuel grate. This meant that the biochar, as the solid pyrolytic

product, was also gasified in order to obtain emissions data of all combustion phases.

Natural draft as well as various forced draft primary air flow configurations were tested in the present study. For the natural draft case, all sides of the primary air inlet chamber were open, as shown in Figure 2 and air could enter the furnace freely. In the forced draft configuration, the sides of the primary air inlet chamber were closed off and controlled air flows of 0.048, 0.059, 0.071 and 0.083 kg $m^{-2}s^{-1}$ respectively, were introduced into the furnace from the start of each test, as presented in Table 1. These air flow values were chosen as they should provide an oxygen-limited environment for the migrating pyrolysis, in accordance with previous studies on fixed bed reactors [27, 28, 29, 30, 31]. The same testing procedure was used for the natural draft and forced primary air configurations.

2.4. The tested fuel

The fuel for each test consisted of Radiata Pine (*Pinus radiata*) wood chips obtained, in 2014, from various locations across the Mt Lofty ranges of South Australia. They were sourced in-bulk, as pre-chipped material, and sieved through a 25 mm aperture, resulting in an average particle size of 24 mm × 8 mm × 3 mm (length × width × height). The bulk density of the fuel is approximately 210 kg m^{-3}. To avoid the influence of the wood chips' differing moisture content on the burning rate and the emissions [21], all the chips were dried to achieve a uniform moisture content throughout testing. This was done by keeping them for 16 hours in a confined space at a constant temperature of 37 °C, created by an air conditioning unit. The drying process resulted in a fuel moisture content of approximately 7%, as determined by the American Society for Testing and Materials (ASTM) D4442-92(2003) standard procedure [32].

3. Results

Preliminary results were gathered through visual assessment. In further tests, emissions and temperature profiles were also recorded. By relating all the findings (visual, emissions and temperature measurements) to one another, a full picture of the process can be drawn.

3.1. Visual Assessment

For the visual assessment, the stove extension was not connected to the stove body. This meant that the gasification products were burned as a non-premixed jet flame, issuing from the stove body into the surrounding air, which could, in turn, be observed without obstruction. Visual assessment is a powerful tool, especially for on-site use where other tools might not be available. Here it is applied to present and discuss visual indicators that can be observed in TLUD combustion. The key features are illustrated in Figure 4.

After lighting, combustion takes place directly at the fuel-stack. This can be seen by flames spreading from the kindling material over the surface of the biomass. Once the upper layer of the fuel-stack is ignited, the temperature increases and small amounts of smoke start to be released, which can be seen in Figure 4 (a). This suggests that the remaining water in the fuel evaporates and volatile compounds are released from the fuel.

A change can be observed once thick white smoke is released from the fuel-stack, as shown in Figure 4 (b). The thick smoke is subsequently ignited and clean-burning, as displayed in Figure 4 (c). This indicates that a second phase, termed migrating pyrolysis, has begun. In the transition period from the lighting phase to the migrating pyrolysis, increasingly volatile compounds and the remaining moisture are released from the fuel, observable as thick white smoke. This thick white smoke was especially prominent in some cold start tests, where it was observed that the flames on top of the fuel-stack would not ignite a flame at the top of the stove body without an external influence (i.e. it was necessary to light manually), as is presented in the supplementary material.

Once the volatile compounds are ignited, a bright yellow flame establishes that burns very cleanly, as shown in Figure 4 (c). Above the flame, no smoke can be visually observed. The separation between the migrating pyrolysis taking place in the fuel-stack and the pyrolytic products being burned separately in time and location, at the secondary air inlet, is a distinctive characteristic of TLUD stoves [33]. The black char that can be seen on the fuel grate, while the bright yellow flame is present at the top of the stove body, reveals this separation.

The extinction of the flame at the secondary air inlet indicates the end of the migrating pyrolysis phase and the onset of char gasification. This phase begins because insufficient combustible gases are released from the fuel-stack to sustain the flame at the secondary air inlet. Although not presented,

during testing, it could be seen that hot glowing char is left on the fuel grate, with small irregular flames above the char bed. If no more air were supplied or the process were quenched, the biochar, could be collected, as displayed in Figure 4 (d). For the purposes of this research, however, the measurements and assessment of the emissions of the char gasification process are desired. Therefore the process is not ended, and it can be seen that the amount of hot glowing char decreases until only ash remains on the fuel grate.

3.2. Normalisation and mathematical phase separation

As described in Section 2.2, all emissions profiles were normalised to account for the influence of test-specific ambient conditions. This included the calculation of the so-called nominal combustion efficiency (NCE), which is defined as $CO_2/(CO + CO_2)$ [17]. The NCE is a key indicator of the stove's efficiency because it displays the proportion of products of complete combustion over the overall carbon emissions. Therefore the higher the NCE, the cleaner and more efficient the burning process.

Three phases can be identified in each of the four profiles presented in Figure 5. The three phases are the lighting phase, the migrating pyrolysis phase and the char gasification phase. A mathematical separation of these three phases was performed. The combustion process in each phase is different and thus it is important to generate independent averaged data. A change in phase was identified when the temporal derivative of the normalised CO profile exceeded 0.002 s^{-1}. This value was determined following a rigorous verification based on inspection of the profiles and was found to be reliable at identifying each phase. To account for the differences in the combustion behaviour, with steady emissions profiles in the migrating pyrolysis phase as opposed to peak values in the lighting phase and multiple peaks in the char gasification phase, peak values as well as time-weighted-average (TWA) values are calculated. The average peak values were calculated for the lighting phase and the average TWA for the migrating pyrolysis phase. For the char gasification phase, average peak values, as well as average TWA values, were calculated. Table 2 presents the results of the above mentioned calculations with the standard deviation in parentheses underneath.

3.3. Natural draft emissions profiles

It is apparent from Figure 5 (a) that in the lighting phase, the NCE can be extremely low, with one peak reaching below 0.6 compared with an average of 0.9965, as presented in Table 2, in the migrating pyrolysis phase. This

in turn means that there are high amounts of the products of incomplete combustion, seen in the CO and H_2 profiles in Figure 5 (b, c).

At the onset of the migrating pyrolysis phase, a flame-front establishes at the secondary air inlet. The NCE simultaneously rises to an average of 0.9965, which is much higher than in the other phases, while the CO and H_2 emissions remain consistently low. In this phase, the migrating pyrolytic front moves steadily down the fuel-stack, which provides the necessary gaseous products for the flame at the secondary air inlet to be sustained. This phase is highly efficient and exhibits extremely low emissions of incomplete combustion.

In the char gasification phase, CO and H_2 emissions are relatively high, resulting in an NCE as low as 0.8518.

3.4. Natural draft temperature profiles

The temperature profiles, presented in Figure 6, reflect the results from the emissions data. The three phases can be identified, based on the gradient of the temperature profiles. In the lighting phase, the gas temperature inside the stove body heats up much more quickly than in the stove extension because combustion takes place on top of the fuel-stack. Once the migrating pyrolysis phase starts and a flame-front establishes at the secondary air inlet, the gas temperature in the stove extension rises above the gas temperature in the stove body. Towards the end of the migrating pyrolysis phase, when the flame-front at the secondary air inlet extinguishes and combustion starts taking place on top of the fuel bed, the temperature inside the stove body starts increasing until it peaks in the char gasification phase.

3.5. Forced draft profiles

The time frames of the different air configurations are presented in Figure 7. The lowest air flow causes the lighting and char gasification phase to be longer than in the natural draft case, while the migrating pyrolysis phase is shorter. For all configurations, the char gasification phase is longer in the forced draft case, while the lighting and migrating pyrolysis phases are shorter. Thus it can be seen that it is not possible to simulate natural draft conditions by introducing a constant primary air flow. With higher airflows it can be observed that the standard deviation, of the time spent in a phase, subsides significantly leading to a higher repeatability of the test conditions.

The emissions from the system under forced draft conditions are illustrated in Figure 8. In the lighting phase, the normalised peak NCE values are only considerably higher than in the natural draft configuration when the highest primary air flow is provided, and are significantly lower with the lowest air flow. The TWA NCE in the migrating pyrolysis phase is similar in both configurations, around the value of 0.9965 in the natural draft case. In contrast, in the char gasification phase, the influence of an increase in the primary air flow has a visible effect. The TWA NCE steadily falls, with the lower two values of the primary air flow achieving a higher efficiency, than the natural draft case, while the higher two values exhibit a lower efficiency.

A comparison of the emissions profiles in relation to the time frames spent in each phase provides further evidence that natural draft conditions cannot be simulated by introducing a forced primary air flow. The emission profiles of, for example, the migrating pyrolysis phase, in Figure 8 (b), suggest that natural draft similar conditions are achieve with a forced air flow of 0.059kg $m^{-2}s^{-1}$, while the time frames in the phase, in Figure 7 (b), suggest that a lower value than 0.048kg $m^{-2}s^{-1}$ would be necessary. Similarly contradicting results are noted for the lighting and char gasification phase.

4. Discussion

In the lighting phase, the profiles, seen in Figure 5, can be related to the incomplete combustion of the kindling material and the top layer of the biomass. The combustion of the kindling material and the top layer of biomass takes place inside the stove body where the surrounding oxygen is rapidly consumed and insufficient primary air enters through the fuel-stack for complete combustion. As described, this CO peak in the lighting phase had previously been observed to increase with a lower calorific value of the kindling material [24]. Furthermore, it had been detected that the lighting phase contributed a large amount of the overall $PM_{2.5}$ emissions, which can also be the result of incomplete combustion [34]. It should be noted, though, that only three of the eight tests show very high CO peak values, which suggests that consistently lower emissions in this phase could be achieved. These deductions are supported by the results from the forced draft primary air tests, which are presented in Figure 8 (a). It can be seen that the peak NCE rises with higher air flows achieving a maximum value of 0.9631 for the highest air flow, which provides sufficient oxygen inside the stove body for more complete combustion.

The thick smoke, which was observed at the onset of the migrating pyrolysis phase, in Figure 4 (b), indicates that there are high amounts of vaporised pyrolysis products, such as tars, heavier hydrocarbons and water, in the gas stream. This suggests that the process of cracking pyrolytic products into lighter hydrocarbons, which occurs at high temperatures and for which hot char particles act as a catalyst [11, 13] , is restricted. This observable amount of volatile compounds supports the hypothesis that cracking in gasifier-based stoves might be restrained due to the limited char bed thickness above the migrating pyrolysis front, resulting in a very short residence time of pyrolysis products in the char layer [14]. The released combustible products in the migrating pyrolysis phase, which exit the fuel-stack as thick smoke, are only partially oxidised inside the stove body because of the insufficient oxygen supply from the primary air inlet, and rise to the secondary air inlet. At the secondary air inlet, the thick smoke would typically be ignited, once it mixes with oxygen from the entering air, by the flames which were established in the lighting phase on the fuel-stack. This implies that the flames that establish in the lighting phase need to bridge the distance between the fuel-stack and the location where a combustible mixture of secondary air with gasification products from the fuel is present. Cases in which the flames on top of the fuel stack do not bridge this distance to ignite flames at the secondary air inlet were experienced when the stove extension was not connected to the stove body, as presented in the supplementary material, and also in some cold starts, when pre-heating the furnace. This has not previously been observed when testing smaller TLUD stoves and needs to be considered when designing larger TLUD stoves, where the distance between the fuel and the secondary air inlet increases.

Comparing the profiles of the migrating pyrolysis phase, in Figures 5 and 8 (b) with the results of Johnson *et al.* [35] and Jetter *et al.* [17] it can be seen that very few stoves can achieve NCE values of this magnitude. It should be borne in mind, however, that this comparison is limited because Johnson *et al.* [35], presented averages of the NCE over water boiling tests (WBT) and minute-by-minute NCE ratios for normal stove use in homes, while Jetter *et al.* [17] measured the NCE over the high-power (cold start) phases of the WBT. Their results are only compared with the average of the migrating pyrolysis phase of this study. This comparison still verifies the high efficiency of the research furnace and the potential of this type of stove.

During the pyrolysis phase the endothermic reactions inside the stove body are mainly sustained by the heat released from the gasification of the

pyrolysis products, which causes the temperature at location B to drop, as can be seen in Figure 6. The gas temperature at location B, inside the stove body, reduces to below 400 °C, which means that the temperature of the pyrolysis products, once they reach the secondary air inlet, will be below this value. This drop of pyrolysis product temperature from ≈ 600 °C , when leaving the fuel bed [15] , to below 400 °C when reaching the secondary air inlet, suggests a cooling effect. This cooling effect can be assumed to be due to a combination of endothermic reactions of the gasification products and the heat loss through the furnace walls. Reducing this heat loss, either by insulating the stove body or by using released heat from the outer surface of the combustion chamber to pre-heat the secondary air, as is done in some TLUD designs, could further influence the combustion at the secondary air inlet positively.

The high CO emissions, which can be observed in the char gasification phase in Figure 5 and Figure 8 (c) , were to be expected and had previously been detected [15]. An increase in the surface oxidation due to a higher relative surface area of the char particles can be assumed to cause these high CO emissions [36]. The lower NCE with a higher primary air flow, as seen in Figure 8 (c), could be a result of more CO, the main gasification product, being transported out of the high temperature reaction zone of the char bed before being fully oxidised. This conclusion is supported by the results from the natural draft case. The highest CO emissions, as presented in Figure 5 (b), were measured when the gas temperatures inside the stove, as illustrated in Figure 6, were at their peak, thus when it can be assumed that the buoyancy force, and in turn the primary air flow, was at its greatest.

The high H_2 emissions in the char gasification phase, in Figure 5 (c), should also be noted carefully because they cannot necessarily be explained by char gasification. These emissions might indicate that the release of hydrocarbons in the migrating pyrolysis phase is incomplete. Therefore it might be possible, through further study, to optimise the migrating pyrolysis phase to achieve a higher overall efficiency of TLUD stoves.

5. Conclusions

In order to better understand the combustion process in TLUD stoves, and to enable future optimisation of TLUD designs for various conditions, a research furnace has been commissioned. In the lighting phase, high primary air flows lead to an increase in peak NCE values and are therefore desir-

able to reduce emissions of incomplete combustion during this phase. In the migrating pyrolysis phase, an increase in forced primary air flows has little advantage over natural draft conditions in terms of NCE values, but lower primary air flows lead to higher CO emissions.

In the char gasification phase, the NCE values are significantly higher with low forced draft primary air flows, as compared with natural draft or with high forced draft primary air flows, due to the reduced residence time within the high temperature reaction zone of the char be facilitating less complete oxidation to CO_2. These findings demonstrate that high controllability of the air flow in each of the distinct combustion phases of a TLUD enables an improvement in the efficiency of the combustion system and a reduction in the emissions of incomplete combustion.

6. Acknowledgements

The authors wish to acknowledge the support of The University of Adelaide and Marc Simpson, the laboratory facilities manager. The contributions to the provision and analysis of the experiments by Aleksis Xenophon, James Metcalfe and Oliver Robson are greatly appreciated.

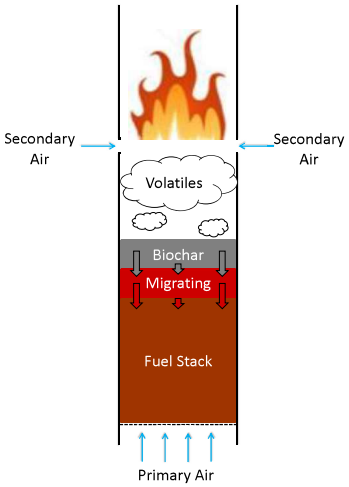

Figure 1: Schematic diagram of TLUD operation.

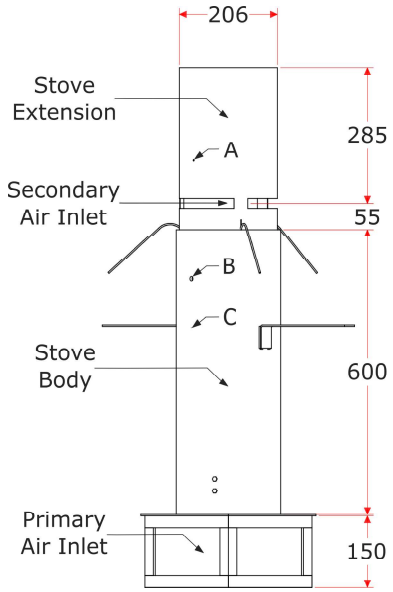

Figure 2: Schematic TLUD research furnace configuration for natural draft conditions (all measurements in millimetres).

Table 1: Air flow and repetitions of the different test configurations

	Repetitions	Primary air flow(kg $m^{-2}s^{-1}$)
Natural draft	8	Natural draft
Varying	5	0.0472
primary air	4	0.0590
	6	0.0708
	6	0.0826

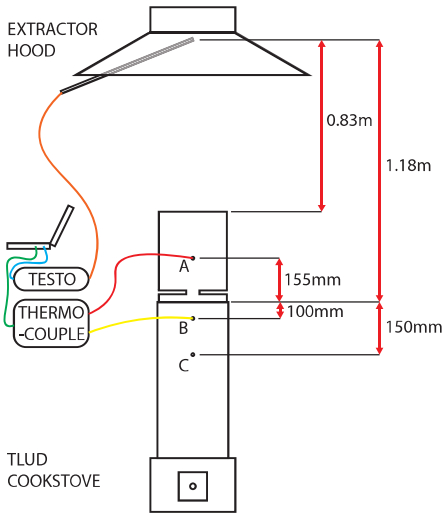

Figure 3: Data collection set-up of the TLUD research furnace.

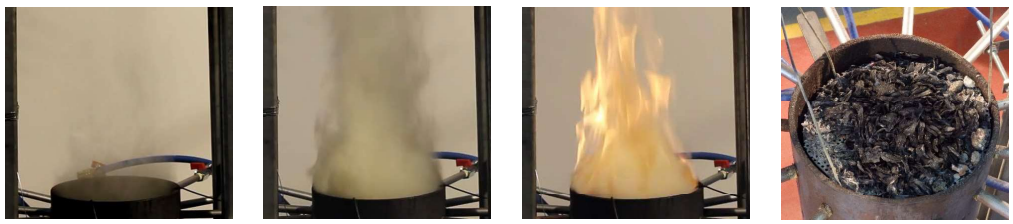

(a) (b) (c) (d)

Figure 4: Visual assessment: a) smoke starts to be released, b) thick smoke rising from fuel-stack prior to ignition of gaseous products, c) combustion of volatiles after mixing with secondary air, d) remaining biochar.

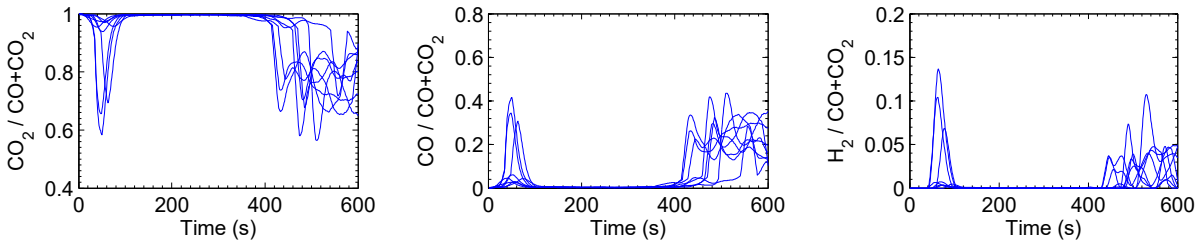

(a) NCE (b) Normalised CO Traces (c) Normalised H_2 Traces

Figure 5: Normalised emissions data of CO_2, CO and H_2 measurements for eight individual tests.

	Lighting	Migrating pyrolysis	Char gasification
Time in Phase [s]	95.1	285.4	221.5
	(9.9)	(27.7)	(17.1)
Minimum NCE peak	0.8404	–	0.6572
	(0.1658)	–	(0.0569)
Maximum $CO/(CO_2 + CO)$ peak	0.1596	–	0.3428
	(0.1658)	–	(0.0569)
Maximum $H_2/(CO_2 + CO)$ peak	0.0418	–	0.0556
	(0.0538)	–	(0.0240)
TWA - NCE	–	0.9965	0.8518
	–	(0.0006)	(0.0427)
TWA - $CO/(CO_2 + CO)$	–	0.0035	0.1482
	–	(0.0006)	(0.0427)
TWA - $H_2/(CO_2 + CO)$	–	0.00013	0.01368
	–	(0.00015)	(0.00727)

Table 2: Averaged normalised peak values and time-weighted-average (TWA) values for the three phases, with the standard deviation of eight repeat tests in parentheses underneath

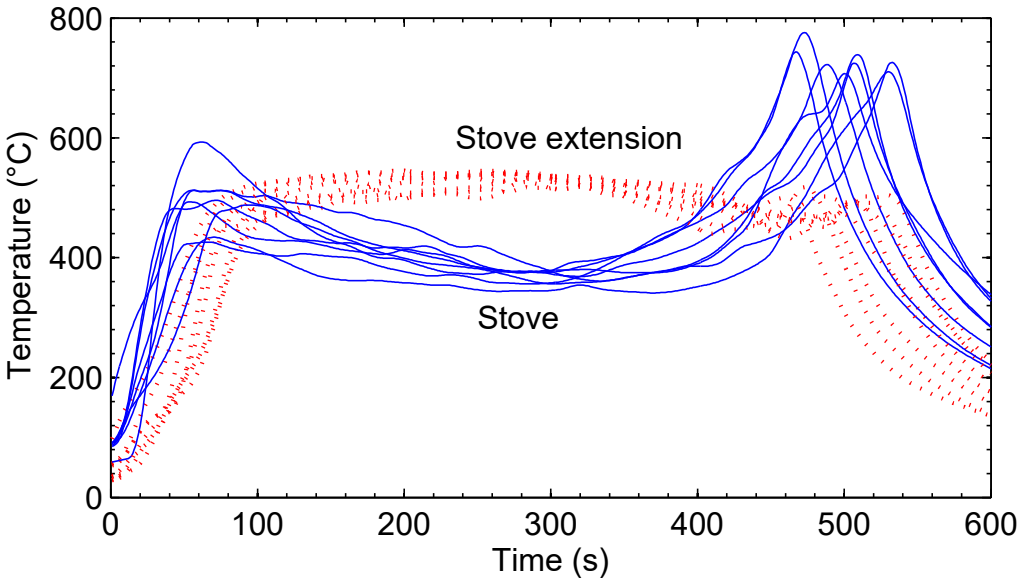

Figure 6: Mean temperatures in the stove and in the stove extension.

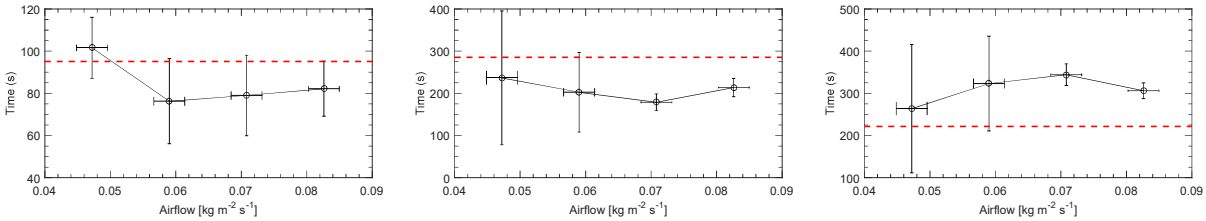

(a) Lighting phase (b) Migrating pyrolysis (c) Char gasification

Figure 7: Average time of the three phases of TLUD combustion with various forced primary air flows compared with natural draft conditions. The red dotted line demonstrates the respective result from the natural draft configuration.

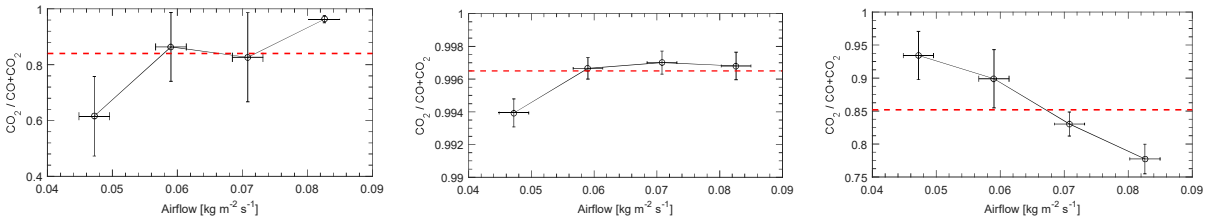

(a) Lighting phase (b) Migrating pyrolysis (c) Char gasification

Figure 8: Average peak nominal combustion efficiency (NCE) values for the lighting phase and time-weighed-average NCE values for the migrating pyrolysis and char gasification phase of various forced primary air flows compared with natural draft conditions of TLUD combustion. The red dotted line demonstrates the respective result from the natural draft configuration.

Figure 9: Thick white smoke can be observed issuing from the stove body which was especially prominent in some cold start tests. It can be observed that the flames on top of the fuel-stack do not ignite a flame at the top of the stove body without an external influence, i.e. it is necessary to light manually. Subsequently the gasification products are burned as a non-premixed jet flame.

7. References

[1] Bonjour, S., Adair-Rohani, H., Wolf, J., Bruce, N.G., Mehta, S., Prüss-Ustün, A., et al. Solid fuel use for household cooking: Country and regional estimates for 1980-2010. Environmental Health Perspectives 2013;121(7):784–790.

[2] WHO, . Household air pollution and health - Fact sheet N 292. 2014. URL: http://www.who.int/mediacentre/factsheets/fs292/en/.

[3] Smith, K.R., McCracken, J.P., Weber, M.W., Hubbard, A., Jenny, A., Thompson, L.M., et al. Effect of reduction in household air pollution on childhood pneumonia in Guatemala (RESPIRE): A randomised controlled trial. The Lancet 2011;378:1717–1726.

[4] Baumgartner, J., Smith, K.R., Chockalingam, A.. Reducing CVD through improvements in household energy: Implications for policy-relevant research. Global Heart 2012;7(3):243–247.

[5] Simon, G.L., Bailis, R., Baumgartner, J., Hyman, J., Laurent, A.. Current debates and future research needs in the clean cookstove sector. Energy for Sustainable Development 2014;20:49–57.

[6] Anderson, P.S., Reed, T.B.. Biomass Gasification: Clean Residential Stoves, Commercial Power Generation, and Global Impacts. In: LAM-NET Project International Workshop. Viña del Mar, Chile; 2004,.

[7] Sutar, K.B., Kohli, S., Ravi, M.R., Ray, A.. Biomass cookstoves : A review of technical aspects. Renewable and Sustainable Energy Reviews 2015;41:1128–1166.

[8] Kirubakaran, V., Sivaramakrishnan, V., Nalini, R., Sekar, T., Premalatha, M., Subramanian, P.. A review on gasification of biomass. Renewable and Sustainable Energy Reviews 2009;13(1):179–186.

[9] Roth, C.. Micro-gasification : cooking with gas from dry biomass. 2014. URL: http://www.giz.de/fachexpertise/downloads/giz2014-en-micro-gasification-manual-hera.pdf.

[10] Reed, T., Walt, R., Ellis, S., Das, A., Deutch, S.. Superficial Velocity - the Key To Downdraft Gasification. In: 4th Biomass Conference of the Americas. Oakland, California; 1999, p. 1–8.

[11] Basu, P.. Pyrolysis. In: Biomass Gasification, Pyrolysis and Torrefaction; chap. 5; second ed. Elsevier Inc.; 2013, p. 147–176.

[12] Bridgwater, A.. Renewable fuels and chemicals by thermal processing of biomass. Chemical Engineering Journal 2003;91(2-3):87–102.

[13] Basu, P.. Tar Production and Destruction. In: Biomass Gasification and Pyrolysis; chap. 6; second ed. Elsevier Inc.; 2013, p. 177–198.

[14] Varunkumar, S., Rajan, N.K.S., Mukunda, H.S.. Experimental and computational studies on a gasifier based stove. Energy Conversion and Management 2012;53(1):135–141.

[15] Mukunda, H.S., Dasappa, S., Paul, P.J., Rajan, N.K.S., Yagnaraman, M., Ravi Kumar, D., et al. Gasifier stoves - science, technology and field outreach. Current Science 2010;98(5):627–638.

[16] Raman, P., Murali, J., Sakthivadivel, D., Vigneswaran, V.S.. Performance evaluation of three types of forced draft cook stoves using fuel wood and coconut shell. Biomass and Bioenergy 2013;49:333–340.

[17] Jetter, J., Zhao, Y., Smith, K.R., Khan, B., Yelverton, T., DeCarlo, P., et al. Pollutant emissions and energy efficiency under controlled conditions for household biomass cookstoves and implications for metrics useful in setting international test standards. Environmental Science and Technology 2012;46(19):10827–10834.

[18] Jetter, J.J., Kariher, P.. Solid-fuel household cook stoves: Characterization of performance and emissions. Biomass and Bioenergy 2009;33(2):294–305.

[19] Birzer, C., Medwell, P., MacFarlane, G., Read, M., Wilkey, J., Higgins, M., et al. A Biochar-producing, Dung-burning Cookstove for Humanitarian Purposes. Procedia Engineering 2014;78:243–249.

[20] Tryner, J., Willson, B.D., Marchese, A.J.. The effects of fuel type and stove design on emissions and efficiency of natural-draft semi-gasifier biomass cookstoves. Energy for Sustainable Development 2014;23:99–109.

[21] Huangfu, Y., Li, H., Chen, X., Xue, C., Chen, C., Liu, G.. Effects of moisture content in fuel on thermal performance and emission of biomass semi-gasified cookstove. Energy for Sustainable Development 2014;21(1):60–65.

[22] Reed, T.B., Anselmo, E., Kircher, K.. Testing & Modeling the Wood-Gas Turbo Stove. Progresss in Thermochemical Biomass Conversion Conference 2000;:693 – 704.

[23] Părpărită, E., Brebu, M., Azhar Uddin, M., Yanik, J., Vasile, C.. Pyrolysis behaviors of various biomasses. Polymer Degradation and Stability 2014;100(1):1–9.

[24] Arora, P., Das, P., Jain, S., Kishore, V.V.N.. A laboratory based comparative study of Indian biomass cookstove testing protocol and water boiling test. Energy for Sustainable Development 2014;21(1):81–88.

[25] Kirch, T., Medwell, P.R., Birzer, C., Holden, L.. The role fo primary and secondary air on wood combustion in cookstoves. International Journal of Sustainable Energy 2016;doi:10.1080/14786451.2016.1166110.

[26] Kumar, M., Kumar, S., Tyagi, S.. Design, development and technological advancement in the biomass cookstoves: A review. Renewable and Sustainable Energy Reviews 2013;26:265–285.

[27] Fatehi, M., Kaviany, M.. Adiabatic reverse combustion in a packed bed. Combustion and Flame 1994;99(1):1–17.

[28] Rönnbäck, M., Axell, M., Gustavsson, L., Thunman, H., Lecher, B.. Combustion processes in a biomass fuel bed - Experimental results. In: Bridgwater, A.V., editor. Progress in Thermochemical Biomass Conversion; chap. 59. Oxford, UK: Blackwell Science Ltd; 2001, p. 743–757.

[29] Horttanainen, M., Saastamoinen, J., Sarkomaa, P.. Operational limits of ignition front propagation against airflow in packed beds of different wood fuels. Energy and Fuels 2002;16(3):676–686.

[30] Porteiro, J., Patiño, D., Collazo, J., Granada, E., Moran, J., Miguez, J.L.. Experimental analysis of the ignition front propagation of several biomass fuels in a fixed-bed combustor. Fuel 2010;89(1):26–35.

[31] Porteiro, J., Patiño, D., Moran, J., Granada, E.. Study of a fixed-bed biomass combustor: Influential parameters on ignition front propagation using parametric analysis. Energy and Fuels 2010;24(7):3890–3897.

[32] American Society for Testing and Materials, . ASTM D4442-92(2003): Standard Test Methods for Direct Moisture Content Measurement of Wood and Wood-based Materials. 2003.

[33] Anderson, P.S., Reed, T.B., Wever, P.W.. Micro-Gasification: What it is and why it works. Boiling Point 2007;53(53):35–37.

[34] Carter, E.M., Shan, M., Yang, X., Li, J., Baumgartner, J.. Pollutant emissions and energy efficiency of chinese gasifier cooking stoves and implications for future intervention studies. Environmental Science and Technology 2014;48(11):6461–6467.

[35] Johnson, M., Edwards, R., Berrueta, V., Masera, O.. New approaches to performance testing of improved cookstoves. Environmental Science and Technology 2010;44(1):368–374.

[36] Arora, P.S., Jain, S.. Estimation of organic and elemental carbon emitted from wood burning in traditional and improved cookstoves using controlled cooking test. Environmental Science & Technology 2015;49:3958–3965.